ADVANCED INTELLIGENT SYSTEMS
Open Access
www.advintellsyst.com

A Modular Robotic Platform for Biological Research: Cell Culture Automation and Remote Experimentation

*Jungmin Hamm, Seonghyeon Lim, Jiae Park, Jiwon Kang, Injun Lee, Yoongeun Lee, Jiseok Kang, Youngjun Jo, Jaejin Lee, Seoyeong Lee, Monica Cahyaning Ratri, Albertus Ivan Brilian, Seungyeon Lee, Seokhwan Jeong, and Kwanwoo Shin**

Robotic arms are now commonplace in diverse settings and are poised to play a crucial role in automating laboratory tasks. However, biological experiments remain challenging for automation due to their dependence on human factors, such as researchers' skills and experience. This article introduces robotic automation and remote control for both general and biological research tasks through a modularized platform comprising a robotic arm, auxiliary tools, and software. This platform facilitates fully automated or remote execution of key experiments in chemistry and biology, including liquid handling, mixing, cell seeding, culturing, and genetic manipulation. The robot interfaces seamlessly with standard laboratory equipment and operates remotely in real time through an online program. Integration of a vision system via robotic arm webcams ensures precise positioning and object localization, enhancing accuracy. This modularized robotic platform signifies a substantial advancement in lab automation, promising enhanced efficiency, reproducibility, and scientific progress compared to human-led experiments.

1. Introduction

The utilization of factory automation technology with robots, extensively employed in the assembly of machine parts, has witnessed significant advancements in recent years. Its application is now expanding across various industries, including agriculture and logistics.[1–3] In manufacturing, robots are commonly used for tasks that involve repetitive actions such as welding, transportation, and assembly.[4,5] There is a growing demand for robots in the medical field, particularly for high-precision tasks that go beyond simple repetitive actions. Numerous studies are being conducted to explore the utilization of robotic arms in remote surgeries and rehabilitation therapies, often incorporating robot suits.[6–8] Robotic arms are attracting considerable attention among various robot systems due to their cost-effectiveness and versatility across diverse applications. They offer multifunctionality, adaptability to different settings, spatial flexibility resembling human arms, delicate finger movements, and the ability to intuitively mimic human behavior. Equipped with various types of interfaces, such as grippers for interacting with target machines, cameras to perceive the surrounding space and movement, and tactile sensors to transmit touch or gripping actions, robot arms can perform a wide range of tasks as a substitute for human actions.[9]

Lab automation is gaining significant attention in laboratories that handle chemical reagents or biological samples. In this context, robot arms are used for various tasks, including simple switch operations and sample movement. One of the most frequently performed steps in lab automation for chemistry and biology laboratories is liquid dispensing. It involves dividing reagents into multiple aliquots, distributing and mixing various solvents for dilution, preparing specific concentrations, and mixing liquids to initiate chemical reactions.[10] By automating liquid dispensing, researchers can greatly increase the sample processing capacity in their daily work. Consequently, liquid dispensers have been widely developed for laboratory automation. The most common approach involves the repetitive movement of multiple automated pipettes or syringes, which distribute liquid into preset vials by traversing specific intervals.[11]

Typically, a robot arm, however, has six degrees of freedom, mimicking the human arm, and is operated through a gripper attached at its end. The six degrees of freedom in the joints of a robot arm are not suitable for systems that require high-throughput sample preparation, including liquid dispensing.

J. Hamm, S. Lim, J. Park, J. Kang, I. Lee, Y. Lee, J. Kang, Y. Jo, J. Lee, S. Lee, M. C. Ratri, A. I. Brilian, S. Lee, K. Shin
Department of Chemistry and Institute of Biological Interfaces
Sogang University
Seoul 04107, South Korea
E-mail: kwshin@sogang.ac.kr

S. Lim, I. Lee, Y. Lee, J. Kang, Y. Jo, J. Lee, S. Jeong
Department of Mechanical Engineering
Sogang University
Seoul 04107, South Korea

M. C. Ratri
Chemistry Education Study Program
Sanata Dharma University
Yogyakarta 55281, Indonesia

The ORCID identification number(s) for the author(s) of this article can be found under https://doi.org/10.1002/aisy.202300566.

DOI: 10.1002/aisy.202300566

However, they can be used for specific liquid distribution requirements. In fact, Lego liquid handling robots using R3 Lego Mindstorms[12] and open-source DIY liquid handling robots[13] have been introduced. These robots have volumetric resolutions of 2.5 and 20 μL, respectively. While these robots can be assembled by the user, their accuracy and reliability may vary depending on the expertise and technical level of the builder. Recently, Knobbe et al. developed a robot system with two robot arms and two grippers using standard laboratory equipment, micropipettes.[14] This robot can handle liquids ranging from 10 to 1000 μL and is operated precisely according to ISO 8655 standards.

However, applying a single robot arm to execute cascade tasks involving sequences of completely different motions in a serial and continuous manner proves to be extremely challenging, extending beyond the scope of repetitive tasks. A single interface is designed to accommodate only a limited range of hand movements achievable with human fingers, which makes it difficult to securely access various tools optimized for human hands. In this regard, although the mentioned research has developed a robot arm, it falls significantly short when directly compared to dedicated automated machines designed solely for liquid dispensing functions.

In recent times, there has been a strong demand for the development of remote-controlled work environments due to educational needs, such as remote experiments, in environments like pandemics. Additionally, the integration of advanced technologies like machine learning is increasing the number of automation applications.[15] With improvements in control and sensor systems and the decreasing cost of robot arms, this trend is expected to continue, leading to more application cases.[16,17] However, as of now, there have been no reported technologies utilizing robot arm systems that can replace the functions and processes of other laboratory tasks routinely performed by skilled researchers, except for liquid dispensing or simple equipment manipulation.

In biology experiments at the university laboratory level, skilled human researchers use various manually operated devices to conduct a wide range of experiments.[18] For example, even basic biology experiments like cell culture require researchers to utilize a variety of familiar tools.[19,20] These experiments involve several complex steps and manipulations, including: 1) Preparation of solutions such as phosphate buffere saline (PBS), media, and trypsin for cell culture. This requires the use of various tools such as beakers, measuring cylinders, and conical flasks of different sizes. 2) Liquid handling tasks involving the distribution, mixing, and dilution of various solutions. Precise pipettes for volumes of 10, 100, and 1000 μL, pipette tip exchange systems, magnetic stirrers, and stir bars are necessary for these tasks. 3) Operating various equipment such as incubators, conical tubes, centrifuges, heaters, etc., with on–off functionality. and 4) Performing cell thawing, seeding, transplantation, counting, and observation using a microscope.

Skilled researchers are trained to perform these complex procedures without errors through repetitive experiments. However, designing a mechanical robot arm capable of executing all these intricate processes accurately remains highly challenging.[18,21]

In this article, we have developed a robotic platform comprising robot arms, auxiliary devices, and software that enables the automation or remote operation of various types of chemical or biological experiments commonly performed in university laboratories. This modularized platform facilitates easy application to different experiments according to protocols. It demonstrates the capability to perform the entire experimental process using a single robot arm, from precise liquid dispensing and mixing to cell seeding, actual cell culture, and even genetic manipulation. The devices used on the platform can be operated remotely from an external location. It allows for remote control of experiments based on the researcher's intentions and supports educational cell experiments within preset routines for educational purposes. A vision system, incorporating a webcam for precise position control and object location information, enhances accuracy and minimizes errors. The experimental tools employed, such as glassware, pipettes, and cell culture incubators, are mostly identical to those used by researchers. Furthermore, various interfaces that provide stable connections between the two-finger gripper and these experimental devices are introduced.

2. Results and Discussion

An overview of the major auxiliary apparatuses arranged around a robotic arm named Cellbot (**Figure 1**a), capable of automated cell culturing as a primary function and further enabling gene transfection experiments. In the middle of the optical table, there are seven distinct areas marked with ArUco markers, surrounding a robot arm that rotates 360°. Various auxiliary apparatuses are arranged in these areas. Most of the apparatuses consist of commonly used machines in biology labs, such as incubators, centrifuges, and suctions, along with tools like pipettes and tips, petri dishes, and conical tubes. These devices are arranged without any significant mechanical modifications. These tools are combined with lab-designed interfaces to ensure stable handling even with a single gripper attached to this robot arm. The enlarged photos of these individual devices are shown in Figure 1b.

The robotic arm we used is an automation robot arm called ZEUS ZRA-0503P (Figure 1b (9)), which provides six degrees of spatial freedom through six-axis joints. The gripper is equipped with a USB 2.00 camera for position and tool recognition using preassigned ArUco markers, and it is attached with specially designed fingertip attachments that are suitable for biochemical experimental tools. These fingertip attachments were manufactured using 3D printing and aluminum machining (Figure 1b (8)). Each tool required for cell culture experiments is arranged in a circular manner around the robot arm, maximizing space efficiency.[22] Starting from the top left, there is a CO_2 incubator (Figure 1a (1-i)) for cell storage, a microscope (Figure 1a (1-ii)) for cell observation, a pipette case and holder (Figure 1a (2-i)) connected to a 200 μL pipette, and a pipette tip case (Figure 1a (2-ii)) placed on the platform. A dedicated 250 mL conical tube holder (Figure 1a (3)) for holding solution-filled tubes used in cell culture, a plate stand (Figure 1a (4-i)) for arranging petri dishes at various angles, and a dedicated 100 mL conical tube holder (Figure 1a (4-ii)) are placed at the front. Toward the right of the robotic arm, there is a centrifuge (Figure 1a (5-i)), an aspirator for liquid suction (Figure 1a (5-ii)), a

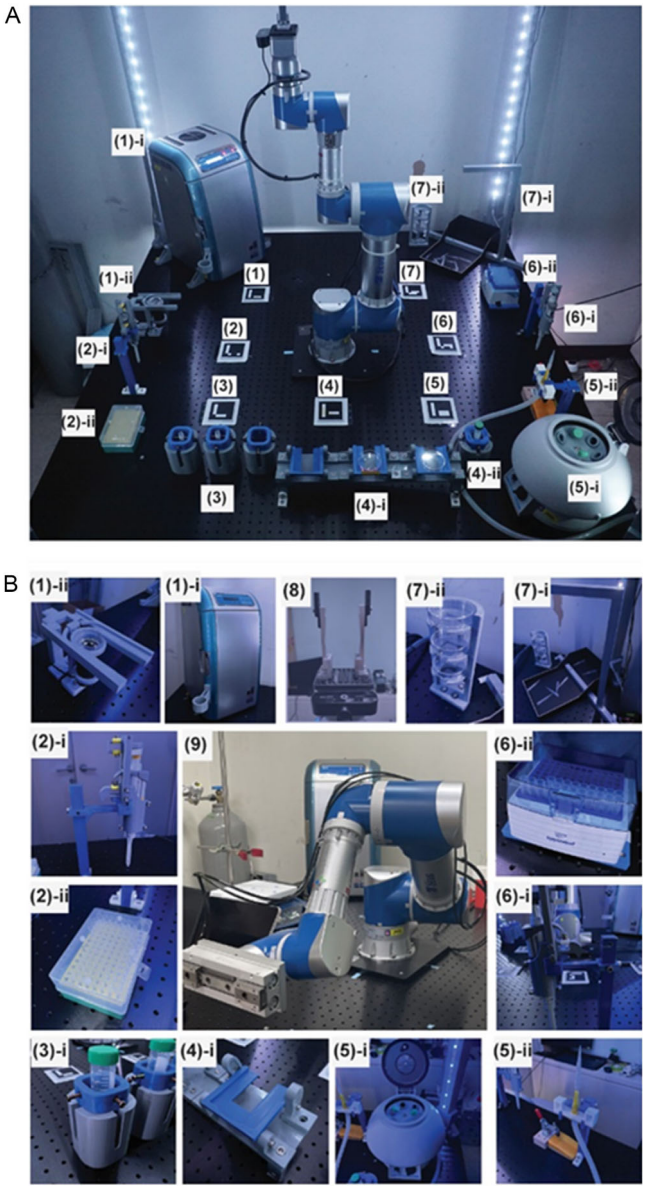

Figure 1. A robotic arm platform enabling cell culturing and gene transfection. A) Foreground view of the ZRA-0503P 6-axis robotic arm with custom-made interfaces for experimental tools grouped into seven (1–7) zones using ArUco markers. Zone (1) includes a CO_2 incubator (1-i) and a microscope (1-ii). Zone (2) contains a 200 µL pipette holder (2-i) and its tip rack (2-ii), while zone (3) has three conical tube holders. Zone (4) consists of three dish stands (4-i) and a 15 mL conical tube rack (4-ii). Zone (5) contains a centrifuge (5-i) and a suction machine (5-ii). Zone (6) includes a 1000 µL pipette holder (6-i) and its tip rack (6-ii), while zone (7) houses a pipette tip remover (7-i) and a plate drawer (7-ii). B) These close-up photos from (1) to (7) showcase the combination of experimental tools, such as pipettes, conical tubes, tips, and petri dishes, with these holders and interfaces, installed for use in experiments, (8) fingertip attachments were manufactured using 3D printing and aluminum machining and (9) an automation robot arm called ZEUS ZRA-0503P.

pipette case and holder (Figure 1a (6-i)) that can be connected to a 1000 µL pipette, and a tip case (Figure 1a (6-ii)) arranged in order. A tip remover (Figure 1a (7-i)) for removing pipette tips and a dish drawer (Figure 1a (7-ii)) for holding petri dishes are placed at the rear. Through the arrangement of various tools and interfaces, we have developed a platform that allows the **cellbot** to perform the entire process of most biological experiments, such as cell culture and genetic manipulation, remotely.

A collection of sequential images in **Figure 2** illustrates the process of an automated biological experiment using a robotic arm, focusing on three representative key tasks: pipetting, handling a cell culture dish for incubation, and operating a suction device. Each of the actions performed by the robotic arm can also be seen in Videos S1–S3, Supporting Information. The system enables experienced researchers to design different variations of experiments using existing laboratory equipment by mimicking standard experimental procedures with a robotic arm and modularizing each action. Modularizing predefined action functions makes it easy to build an entire experimental protocol by changing only the order and parameters of the action functions. Figure 2a–c and Video S1, Supporting Information show the process of pipetting using an auxiliary pipette housing designed to be compatible with a two-finger gripper so that it can be used without modification to fit a human hand, specifically the five fingers and the palm. Essentially, Figure 2a shows the gripper inserting and lifting a pipette into the hole in the pipette case in the holder, Figure 2b shows the process of attaching a pipette tip to the lifted pipette, and Figure 2c shows the process of aspirating and dispensing liquid using the attached pipette tip. After inserting the tip into the tube containing the desired liquid and spreading the gripper fingers to aspirate the liquid, the robotic arm moves to the target position and holds the tip in place to dispense the liquid. During these operations, the robotic arm compensates for vertical position changes that naturally occur due to changes in the gripping width of the gripper holding the pipette. The algorithm used for such pipetting was organized as shown in Figure S1, Supporting Information, and the positions and procedures are configured according to different needs.

Figure 2d–f and Video S2, Supporting Information depict the operation of the robotic arm when handling and shaking a 35 mm petri dish for cell culture. Figure 2d shows the robotic arm opening the incubator door and extracting the covered petri dish. Figure 2e demonstrates the process of retrieving the dish and placing it in the designated dish holder in preparation for subsequent experimental procedures, such as liquid handling. During the movement, the dish is always kept horizontal, and a two-finger gripper presses the center of the dish vertically to secure both the lid and the plate. Figure 2f captures the robotic arm firmly gripping the dish and shaking it in four basic directions. Finally, Figure 2g–i and Video S3, Supporting Information illustrate the operation of the suction device controlled by the robotic arm. To activate the suction device, the footrest switch, typically operated by the operator's foot, needs to be pressed and maintained. The robotic arm applies continuous pressure on the footrest using a special clamp device, as shown in Figure 2g. Figure 2h demonstrates the detachment of the suction device from the cradle, and Figure 2i shows the precise alignment of the suction tip at the desired position for liquid aspiration. Throughout the process, emphasis has been placed on the utilization of standard laboratory equipment and the imitation capabilities of the robotic arm and gripper, mimicking the operation of skilled researchers in the laboratory. The modular

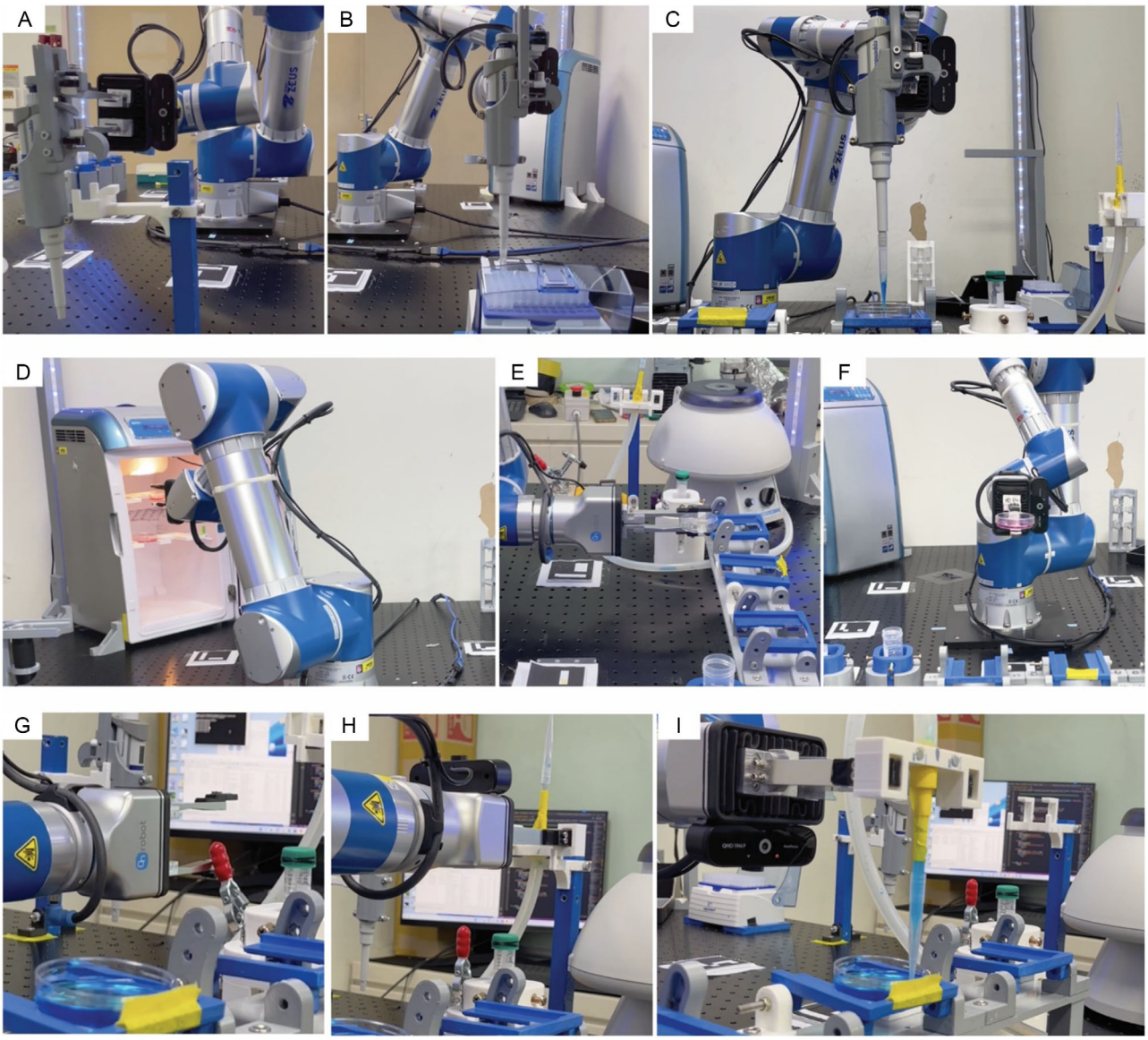

Figure 2. Sequential images of cell culturing experiments using representative experimental tools with a robot arm. A–C) Photos of the 1000 µL pipette being operated in the laboratory using interfaces connected to the robotic arm and a supporting stand. D) Image of removing a dish with culturing cells from the CO_2 cell culture incubator. E) Placing a petri dish on a stand. F) Using the robotic arm to shake the liquid after injection. G–I) Continuous images of using the suction machine to remove liquid from the petri dish.

design of each motion feature ensures flexibility in the experimental setup while guaranteeing universal applicability to various experiments.

Pipetting plays a crucial role in various scientific and laboratory settings, including biology, chemistry, medicine, and research.[23,24] It enables researchers to accurately measure and transfer precise volumes of liquids such as reagents, samples, or solutions for experiments, analyses, or assays. Ensuring reproducibility and accuracy, pipetting is often the starting point for experiments in university chemistry, where the reliability of glassware or pipettes used in the experiment is assessed.[25] **Figure 3**a is the custom-designed 3D design of a pipette housing, serving as an example of the interfaces connecting a robotic arm and a laboratory apparatus. The design comprises five components: top pressing cover, side rails, magnet-equipped finger holes, pipette fastening part, and bottom cover. Two finger holes with magnets simplify use with a two-finger gripper, ensuring steady pipetting. The top pressing cover manually actuates the pipette's plunger button. Side rails adjust the button through three positions—initial, secondary, and release—aligned to gripper force. In Figure 3b (1), 3D-printed devices were combined with various pipettes of different capacities. Robotic fingertips fit into the fingerholes, lifting pipette and case. Dispensing adjusts through gripper width, demonstrated in Figure 3b (2) and (3) and Video S1, Supporting Information. The robotic arm utilized in this experiment was designed with

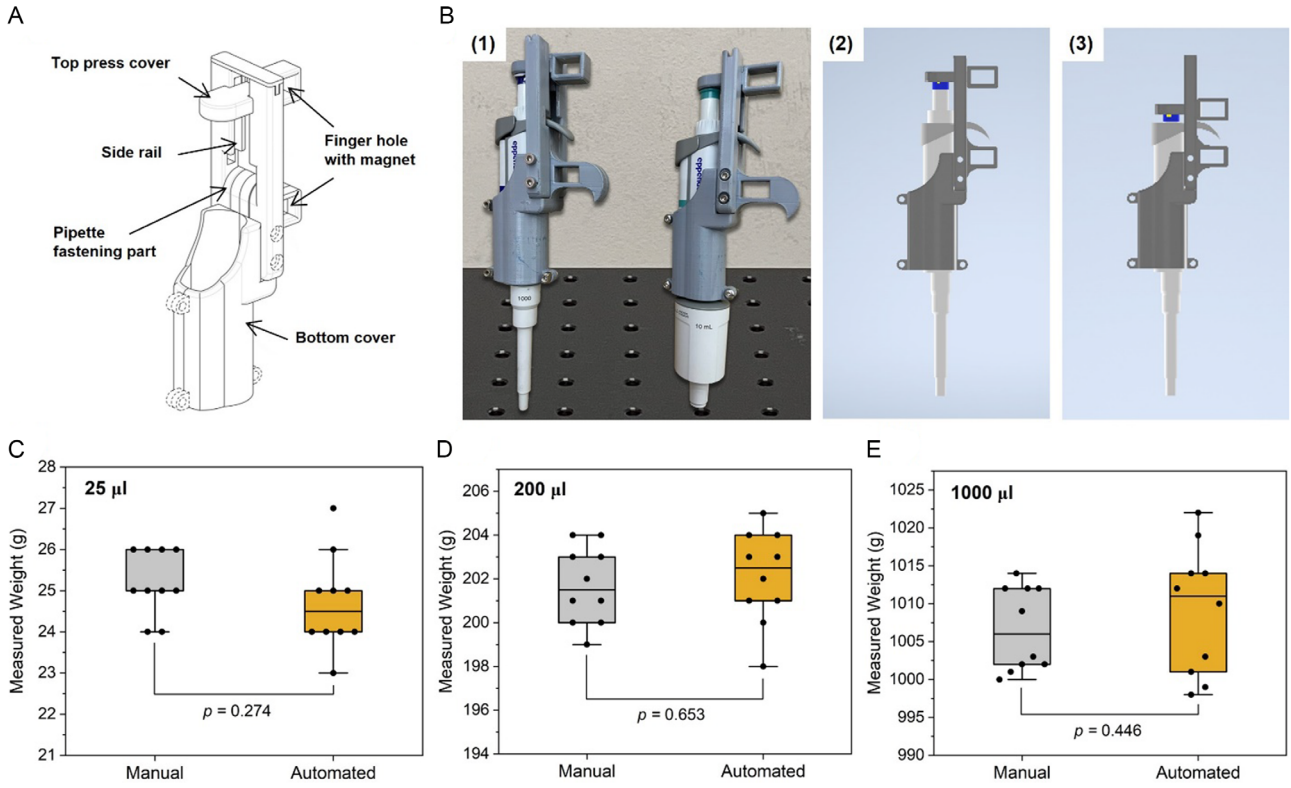

Figure 3. An interface unit connecting a 2-finger gripper with a pipette. A) 3D design of the custom-designed robotic arm housing for pipettes. B) Photos of the holder attached to pipettes (1), operating the interface (2,3). Statistical comparison of the weight of water transferred using the same pipettes with capacities of C) 25 µL, D) 200 µL, and E) 1000 µL both manually and automatically by the robot. A *t*-test was employed for statistical analysis to evaluate the significance of differences between two groups.

a load capacity of 5 kg. Therefore, it is noteworthy that payload capacity was not a concern for most experimental instruments in the lab, including pipette handling. The designed pipette housing weighed around 100 g, and even after mounting, the total weight was ≈185 g.

As this housing was specifically designed for the same pipettes routinely used by humans, we questioned whether disparities in liquid dispensing precision exist between a robotic system and a skilled human operator employing the identical pipette. To evaluate this, a calibration experiment was conducted using water with a density of 0.998 g mL^{-1} at 20 °C. The goal was to assess the ability of the robotic system to handle liquid at a level comparable to human operators, using three types of pipettes: 25, 200, and 1000 µL. The experimental procedure was repeated 10 times for both the manual and automated processes. In the manual process, a researcher performed the pipetting task, while in the automated process, a robot arm equipped with the pipette interface carried out the task. The results revealed that for a 25 µL volume, the error ranges observed in both manual and automated experiments were highly similar (Figure 3c). Although there was a slight increase in overall variability in the automated process, it remained comparable to that of manually pipetted samples. In the case of a 200 µL volume, the automated process exhibited a slightly higher error spread compared to the manual process, but the difference was negligible (Figure 3d). Similarly, for the 1000 µL pipette, the automated process demonstrated a slightly higher error range than the manual process, yet the performance remained comparable (Figure 3e). As depicted in the figures, the *p*-values for all cases significantly exceed 0.05, suggesting that the observed data are not significantly different between the two groups, i.e., manual versus automated. This implies that the robotic arm employed the same pipette as the human, and any variations in the data are more likely attributable to the inherent error range of the pipette rather than differences between the robot and human. Taken together, these results indicate that the developed pipette interface enables the handling of liquids at a level similar to human operators, thereby confirming the utility of the automated system in replacing the skilled human labor in the laboratory while utilizing existing laboratory equipment.

Figure 4 showcases various auxiliary devices developed to enable a robotic arm to utilize laboratory tools and perform a range of experiments in biology and chemistry, including cell culturing and advanced protocols that require precise techniques such as transfection. Typically, trained researchers perform tasks in the lab that require the use of both hands simultaneously. However, those custom-designed devices demonstrate the diverse equipment interfaces designed specifically for conducting the same tasks using only a single six-axis robot arm equipped with a two-finger gripper, ensuring high accuracy

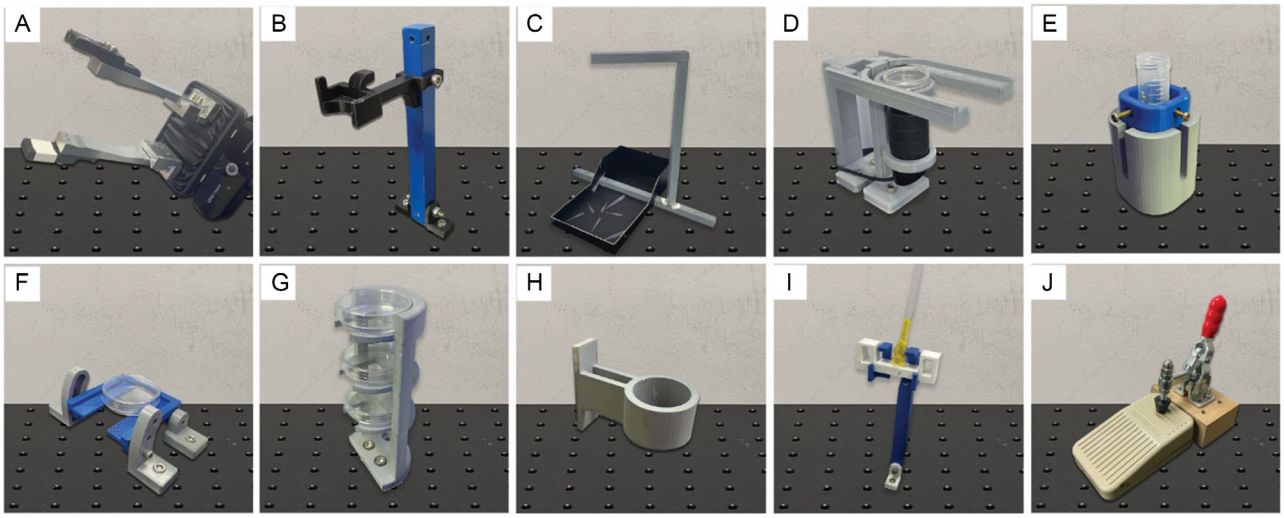

Figure 4. Peripherals and stands enabling the operation of biological experiment tools with a robotic arm: A) end-effector with custom-designed fingertips; B) pipette holder; C) pipette tip remover; D) microscope and dish stand; E) conical tube holder; F) petri dish stand; G) petri dish drawer; H) door handle for opening and closing the CO_2 incubator; I) suction handle and cradle; and J) suction footrest switch and clamp apparatus.

and user-friendliness even with just a two-finger gripper. Many of these devices can be easily produced through 3D printing or simple metal fabrication methods.

First, the end-effector (Figure 4a and S1, Supporting Information) is designed to securely hold objects of different sizes, including glassware such as vials and beakers, as well as pipettes and petri dishes (Videos S4–S6, Supporting Information). It features a 3D-printed fingertip that extends the range of motion of the gripper. This design allows the end-effector to accommodate objects with diverse sizes while maintaining precise control. Additionally, a small magnet is incorporated into the fingertip, enabling the gripper to achieve a precise and stronger grip on the pipette when combined with the magnet attached to the handle of the pipette case.

Auxiliary devices Figure 4b,c further support the use of a pipette. The device (Figure 4b), as detailed in Figure S2 and S3, Supporting Information, serves as a holder for suspending a pipette covered with the interface casing. On the other hand, device (Figure 4c) facilitates the removal of disposable pipette tips by pressing the shoulder of the pipette against the upper bar of the structure (see Videos S7 and S8, Supporting Information). The simple microscope stand (Figure 4d) is designed to securely position a microscope and a cell culture dish for observation, as detailed in Figure S4, Supporting Information. By gently pushing the dish with the gripper finger, it can be brought close to the microscope without any interference.

The conical tube holder (Figure 4e), as also shown in Figure S5, Supporting Information, is designed to prevent the rotation of the tube when the lid is opened while automatically compensating for the vertical movement that occurs as the lid turns along the screw thread. This design allows the robot arm to easily open the lid by rotating a single joint. The holder consists of two parts with a sponge placed between them to facilitate automatic vertical movement compensation. Devices (Figure 4f,g) are a plate stand and a plate drawer, respectively. The plate stand (Figure 4f) allows for angle adjustments of up to 30° in 10° increments, aiding in pipetting and suction (see Figure S6, Supporting Information). The plate drawer (Figure 4g) can store up to three plates for future use, as demonstrated in Video S9, Supporting Information. The incubator handle (Figure 4h), as shown in Figure S7, Supporting Information and demonstrated in Video S10, Supporting Information, is designed to open the incubator door with a simple arc trajectory movement. The gripper finger is inserted into the hole in the handle and moves along a preset arc, enabling easy door opening. Auxiliary devices (Figure 4i,j) assist in the use of a suction device. Device (Figure 4i) is a handle for accurately controlling the position of the suction end and its cradle (Figure S9, Supporting Information). The device (Figure 4j) is a clamp for pressing the suction foot switch, which typically requires constant manual pressure (Figure S9, Supporting Information). Again, this design allows for a single touch to produce the effect of continuously pressing the footrest. Video S11 and S12, Supporting Information, respectively, demonstrate those motions performed by the robot arm.

By utilizing these auxiliary devices, the two-finger gripper has been successfully adapted to effectively handle the experimental equipment typically operated by skilled individuals. The approach employed for each auxiliary device can be further extended to other types of laboratory equipment. By utilizing similar approaches, it is expected that the two-finger gripper can be effectively utilized to operate various types of lab equipment optimized for human use. This opens up the potential for laboratory automation using robots that collaborate with humans, significantly transforming the way experiments are conducted in the lab.

Figure 5 illustrates the process of obtaining and correcting precise coordinate values required for the experiment, focusing on the communication structure and relationships between computer files; Figure 5a is a schematic representation of the

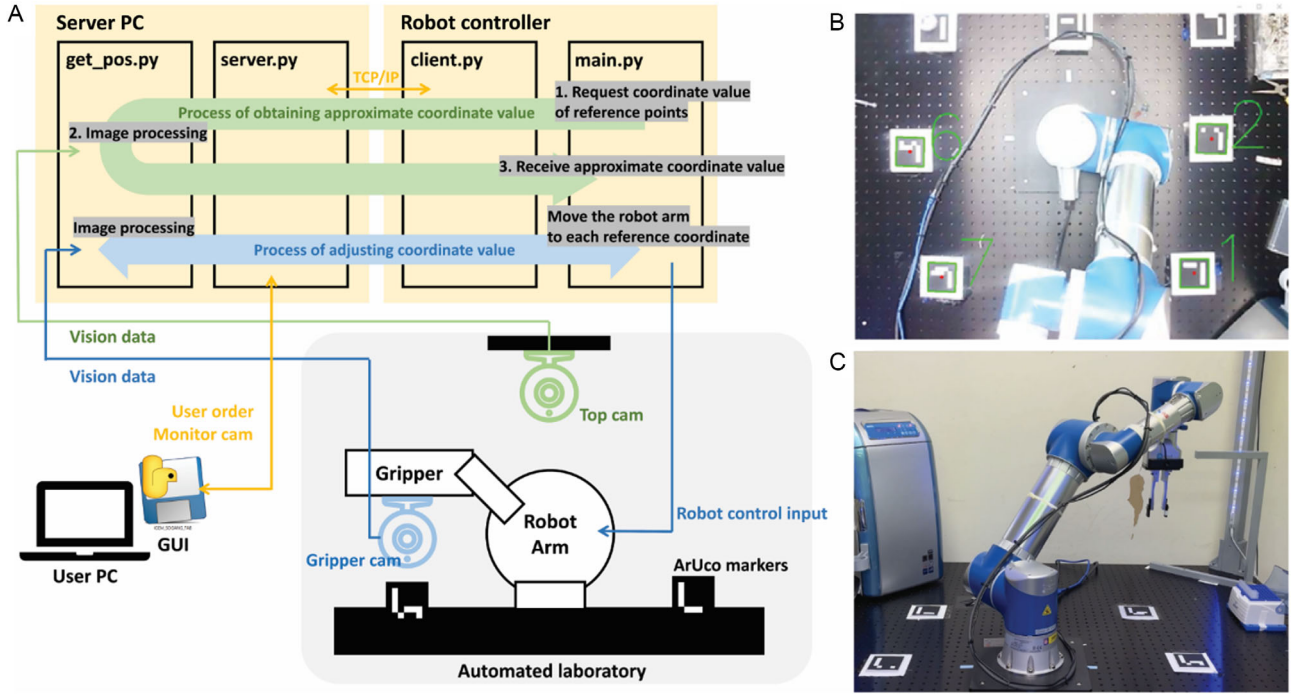

Figure 5. Communication and image processing structure implemented for remote and precise control of robot coordinates. A) Schematic of the communication structure between the robot controller and server PC, along with the communication to user PC with two cameras, Top cam and Gripper cam, to determine accurate coordinate values. B) Image captured from the Top cam to obtain approximate coordinate values. C) Scene showing the robot approaching the coordinates closely for precise measurement using the Gripper cam.

communication structure, Figure 5b is the image captured with a camera mounted on the ceiling of the robotic system (Top_cam) and the arrangement of ArUco markers to obtain approximate coordinate values, and Figure 5c is a photograph depicting the robot closely measuring coordinates using a camera mounted on gripper (Gripper_cam). Due to the constraint of not being able to directly and accurately obtain all coordinate values, a two-step process was adopted to achieve accurate coordinate values. In Figure 5a, the communication structure is presented, consisting of a robot controller and a server PC, along with the two-camera setup for the two-step image processing. The robot controller is responsible for controlling the robot's movement, with the main.py file containing each action function and providing control input to the robot. The client.py file, also part of the robot controller, manages TCP/IP communication with the server PC. The server PC handles image processing, remote communication, and GUI connection. It comprises the server.py file for communication and GUI, and the get_pos.py file for image processing functions specifically for measuring coordinates.

As described earlier, we used ArUco markers with wide black borders to identify the seven experimental modules and estimate the exact coordinates of the placed devices. These markers have an internal binary matrix, which ensures robust, fast, and simple detection and recognition. The first step, as shown in Figure 5b, involves using the top camera mounted on the ceiling to acquire approximate coordinate values for the seven reference coordinates marked with the ArUco markers. This initial acquisition provides a foundation for the subsequent correction process. In the second step, depicted in Figure 5c, the robot closely approaches each reference coordinate and adjusts the coordinate values through up-close measurement using Gripper_cam mounted on the robot's end-effector. By comparing these values with the initially obtained values, the robot calculates the difference between them. The coordinates are then updated based on the calculated difference, and the process is repeated for each reference coordinate. This iterative refinement continues until the difference falls below the 1 mm threshold, ensuring a high degree of accuracy for all reference coordinates. Through this two-step process, positioning accuracy within 1 mm was achieved for all reference coordinates. Additionally, the system was configured for remote access via port forwarding, allowing its use remotely.

We have developed a user-friendly GUI that enables remote users to conduct intended experiments while monitoring the robot's real-time movements. After a simple login (Figure S10a, Supporting Information), the server.py and client.py codes from Figure 5a establish TCP/IP communication for external connections. Users can then choose between Auto-control mode and Step-control mode (Figure S10b, Supporting Information). In Auto-control mode (Figure S11, Supporting Information), the robot automatically performs precisely validated experiments with diverse or sometimes repetitive tasks, using multiple devices like cell seeding, subculturing, and lentivirus transduction, following predefined motions without user intervention. In contrast, Step-control mode (Figure S12, Supporting Information) allows users to selectively control various experimental devices

with different options (i.e., sizes, volumes, or dish positions) as needed.

Video S13 and Figure S13 and S14, Supporting Information display the command process of controlling a cell incubator or opening the lid of a conical tube and the real-time video window of the robot responding to the commands through the GUI. The corresponding buttons developed for each function are listed in Table S2, Supporting Information, providing users with the ability to control various options required for their needs. Using this GUI program, test experiments were successfully performed by remotely accessing the robot platform in Seoul, Korea, from Paris, France. Furthermore, to investigate the educational applications for students in areas where access to school laboratories is difficult during the coronavirus pandemic, undergraduate pharmacy students at Sanata Dharma University in Yogyakarta, Indonesia, were able to successfully perform cell culture experiments via remote access without experiencing any technical delays.

When a long-time trained researcher performs an experiment in the laboratory, they often do not realize how a seemingly simple experiment is a series of elaborate and complex processes, as they are used to performing multiple procedures in an environment optimized for the human body. Even simple tasks that humans perform intuitively are very difficult to recreate with the multiple joints and end-effectors of a programmatically controlled robot. To illustrate the process of translating human motion into robotic motion, we compared the liquid handling procedure of pipetting. **Figure 6**a is a continuous chart comparing the core motion flow of a simplified human and robotic pipetting. The human-operated pipetting process essentially involves: 1) holding the pipette with four fingers and the palm of the hand; 2) inserting the pipette tip; 3) manipulating the plunger button to

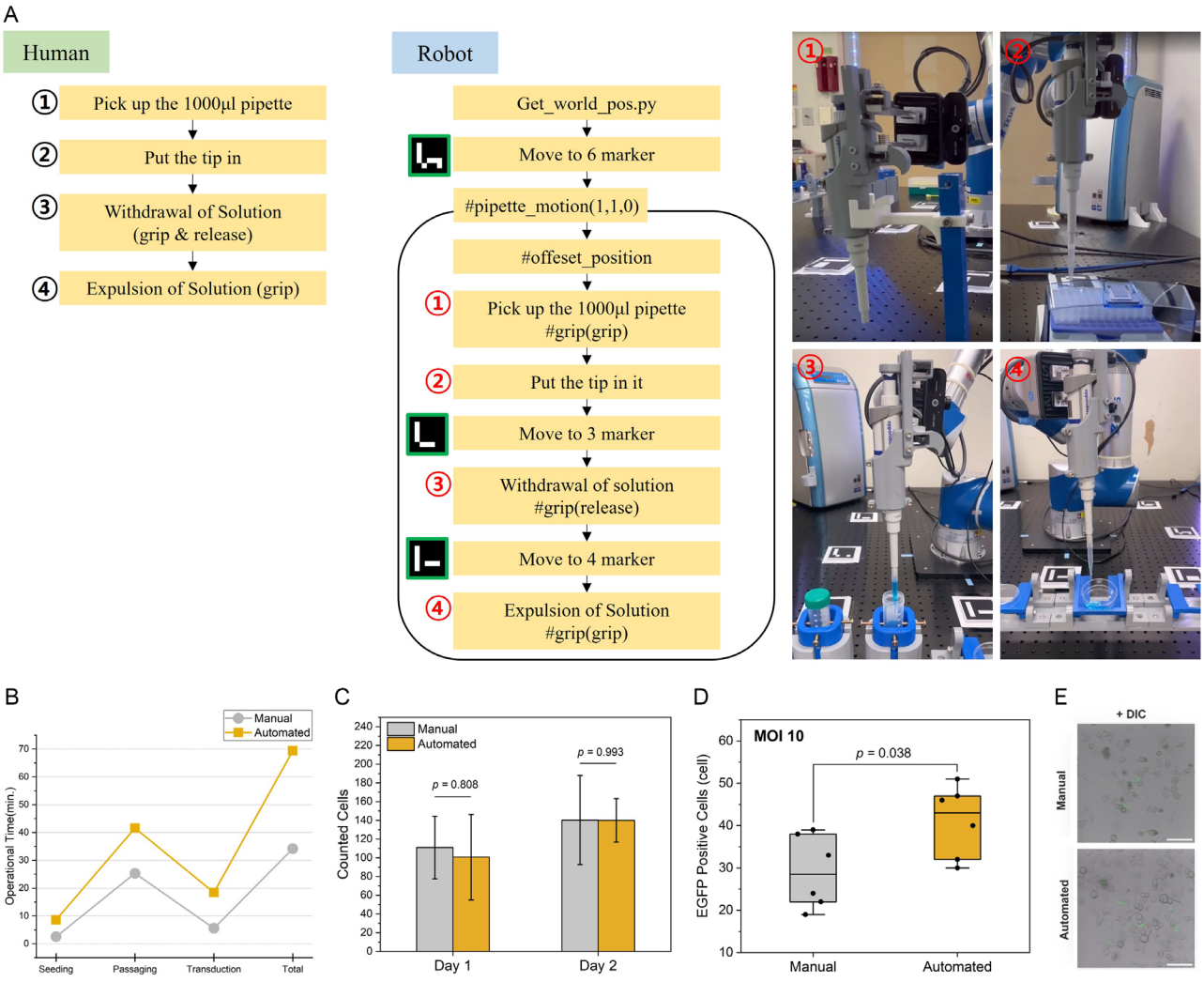

Figure 6. Comparison of human and robot protocols for performing module-specific experiments and results of cell culture and transduction experiments. A) Comparison of human pipetting procedure and robot arm's coded motion flow for pipetting. Progression photos of the robot arm in motion based on pipetting commands. B) Comparison of time taken for cell seeding, passaging, and transduction tasks. C) Comparison of counted cell numbers after HaCaT cell seeding. D) Number of EGFP-positive cells expressing the gene after lentiviral transduction. (C,D) The *t*-test was employed for statistical analysis to evaluate the significance of differences between two groups. E) Fluorescent confocal images of infected cells. Scale bar is 100 µm.

draw in liquid; and 4) dispensing by adjusting the pressure on the thumb. To reproduce this process with the robot's behavior, we can break it down into the following steps: First, accurate coordinate values are obtained using the Get_world_pos.py function to ensure reproducibility of subsequent motions. Then, a series of pipetting motions are performed using the modularized pipette_motion.py function. The robot moves to **Marker** 6, where the 1000 μL pipette is located, and grabs the pipette by offsetting its position by a calibration value. The robot then moves to the tip rack while holding the pipette, inserts the pipette tip, and moves to **Marker** 3, where the conical tube containing the solution is located. The robot then releases its finger to aspirate the solution and moves to **Marker** 4, where the plate is located, and dispenses the aspirated solution into the designated wells. The robot performs additional tasks, such as removing the tip and returning to the pipette at **Marker** 6, following a precise routine without interference from other objects along the way. This sequential process is pictured in Figure 6a. The final routine and coordinates of the robot are optimized by repeated continuous operation to ensure that there is no device-specific interference or error.

At this point, we compared the time taken by our robotic arm to perform various biological experiments with that of an experienced human researcher. For the cell seeding experiment, as shown in Figure 6b and Video S14, Supporting Information, the robot took an average of 8 min and 56 s (SD = ±0.016), while the skilled researcher completed it in an average of 2 min and 52 s (SD = ±0.092). The robot required longer working time compared to humans due to recognizing new initial coordinates at each step and having only one arm. However, it showed consistent time variance in repeated experiments. The more complex cell passaging process took the robot an average of 41 min and 56 s, compared to 25 min and 31 s by hand. Regarding the lentiviral transduction protocol, the robot consistently completed it in an average time of 18 min and 40 s (SD = ±0.014) (see Video S15, Supporting Information). However, this is still 2–3 times longer than humans for experiments that require extended periods of work. Nevertheless, with proper human setup involving pretreatments like preparing different contingencies, we found that the robotic arm can handle tasks like cell seeding, culturing, and gene transfer repeatedly. This approach minimizes errors arising from human experimenter skill and opens up new possibilities for a more precise experimental environment.

Figure 6c shows the number of cultured cells seeded by the manual and automated processes. The cells were continuously observed by confocal microscopy for 2 d starting 24 h after cell seeding. Microscope images captured from culture dishes containing HaCaT cells were extracted and counted using ImageJ software. On the first day (day 1), the automated cell seeding resulted in a slightly lower average cell count and higher standard deviation compared to the manual process (Figure 6c). This may be due to the fact that some cells containing liquid may have been lost during the robot's pipetting process.[26] However, on the second day (day 2), both automated and manual cell seeding had the same average cell count and showed an increase in the number of HaCaT cells. Statistical analysis, conducted using a *t*-test, did not also uncover any significant differences between the two groups. Morphologically, the HaCaT cells appeared healthy and showed no signs of contamination. After transfection, we observed the HaCaT cells using a fluorescence microscope and counted the number of EGFP-positive cells using ImageJ software (Figure 6d). The results showed, however, that the number of infected cells was slightly higher in the automated process compared to the manual process ($p = 0.038$). The successfully transfected HaCaT cells were observed using confocal microscopy with differential interference contrast imaging as a background and showed EGFP expression along with cell morphology (Figure 6e). These results demonstrate the robot's ability to successfully perform lentiviral transduction as part of a biological study.

As a perspective, we would like to highlight a few final steps that researchers need to take when designing experiments using robotic arms for biological tasks, such as gene transfer. First, careful planning is essential, including the selection of auxiliary equipment and programming for control. This involves choosing the appropriate robotic arm and gripper (end effector), integrating it with necessary interfaces, and developing accurate software for controlling the robotic arm's movements. Calibration and protocol definition are crucial for error minimization,[27] along with implementing contamination prevention measures, conducting testing, and validating results before and after gene transfer experiments. Proper training of operators and ongoing maintenance are necessary for optimal performance. Moreover, adhering to biosafety guidelines and involving experts in both biochemistry and mechanical engineering are critical in this delicate and controlled process.

3. Conclusion

In this article, we presented a robotic platform designed to perform chemistry and biology experiments commonly performed in university laboratories, as well as advanced cell biology experiments, either fully automated or customized protocols for different experimental conditions. The platform consists of a robotic arm, auxiliary devices, and software that can be easily adapted to different experiments according to specific protocols. The modularized system demonstrates the ability to execute the entire experimental process with a single robotic arm, including tasks such as liquid dispensing, mixing, cell seeding, culturing, and genetic manipulation. The platform also allows experiments to be controlled remotely from the outside, accommodating researchers' intentions and supporting educational purposes with preset routines for cell experiments. It integrates a vision system with dual webcams for precise positioning and reduced error in object localization, increasing accuracy and reducing undetermined errors during experiments. It can use existing laboratory tools such as glassware, pipettes, and cell culture incubators, ensuring compatibility with existing research practices. The platform also introduces a two-finger gripper and various interfaces to reliably connect experimental devices for seamless operation. Overall, the robotic platform introduced in this article has the potential to significantly impact laboratory automation, driving efficiency, reproducibility, and advancements in the fields of chemistry and biology. The introduction of robots in scientific research and education can foster collaboration and remote experimentation, creating an interconnected scientific research community of robots and humans.

4. Experimental Section

Materials: Dulbecco's Minimum Essential Media (DMEM) (11995065), fetal bovine serum (FBS, 16000044), PBS (10010023), trypsin–EDTA (25200056), and penicillin–streptomycin–glutamine 100x (Pen–Strep, 10378016) were purchased from Gibco. Recombinant lentivirus pLV[Exp]-EGFP/Neo-EF1A>hITGA5[NM_002205.5] (Vector ID: VB900124-1009rmb) and polybrene were purchased from VectorBuilder.

Robot Arm Platform: This robotic arm is the ZRA-0503P model purchased from Global Zeus (Korea). The total arm length is 660 mm, with the first arm measuring 390 mm and the second arm measuring 270 mm. The input power consists of DC 48 V–8 A and DC 24 V–1 A. The total weight is 17.2 kg, and it has a maximum operating range of 660 mm with a load capacity of 5 kg. On this robotic arm, we have installed the 2FG7 parallel gripper purchased from OnRobot (Denmark). All robot setups were used at the Biocore Facility, Institute of Biological Interfaces, Sogang University (Korea). Two sets of LX-V11 USB 2.0 webcams were used. For the cell culture experiments, an IC-20 CO_2 standard incubator and a Cef-6 general-purpose tabletop centrifuge were used. Micropipettes (200 and 1000 µL) from Eppendorf (Germany) and epT.I.P.S 1000 µL tips were also employed, along with 20–200 µL tips from LABCON (USA). The 15 and 50 mL conical tubes from SPL Life Sciences and the 60 mm × 15 mm petri dish from Corning were used. The SMT-01 Suction Master and the SMTOUCHSCOPE smartoy touch digital microscope from Shenzhen Qi Yao Technology Co., Ltd. (China) were utilized. The experimental setup involved using a 1200 × 1200 optical breadboard with M6 bolt holes as a table, with the robot arm positioned at the center and the other auxiliary devices arranged around it. Additionally, an aluminum and steel camera station, along with LED lights, was installed on the table.

3D Printing of Custom-Made Interfaces and Auxiliary Devices: The interfaces were designed using Autodesk Inventor 2023 (Autodesk, USA). Prior to fabrication, stress analysis was conducted using the integrated stress analysis tool provided by Autodesk Inventor to optimize the design, ensuring the interfaces would remain undamaged during interactions with the robot. The native Inventor IPT files were exported from Autodesk Inventor as stereolithography (STL) data. The STL data were then imported into Cura (Ultimaker, The Netherlands), a software that converted the STL data into instructions for the 3D printer to print according to the selected settings. The 3D printer used for the task was the Ultimaker S3 (Ultimaker, The Netherlands). The nozzle was heated to melt and deposit the Tough PLA filament following the calculated pathway. For the physical assembly, aluminum rods, bolts, and nuts of different sizes (M3, M4, and M5) were employed as necessary for constructing parts such as the pipette case, pipette holder, pipette tip remover, conical tube holder, and plate stand. Each of these parts was secured onto the table using M6 bolts.

Control Software: All position control tasks of the robotic arm, including end-tip motions (i.e., orientation and position), were executed using the dedicated controller (ZC1001, Global ZEUS). The control system facilitates high-level position trajectory planning for a given reference, maintaining a repetitive error of ±0.02 mm. The robot motion function code was developed using Python 2.7 and the custom motion library for the ZERO ZRA robot (Global Zeus, Korea). The code is transmitted to the ZERO robot controller via FFFTP.exe and subsequently stored. Communication between the robot controller and the server PC occurs through the transmission control protocol/internet protocol (TCP/IP), facilitating the exchange of commands and image processing information. The server PC acquires the location data of the ArUco marker from a connected webcam (QHD, 5-megapixel) using the Python OpenCV library. Users can remotely access the server PC and control the robot through a graphical user interface (GUI) created with the Python Tkinter module.

Human-Operated Versus Robot-Arm Automated Cell Culturing: Prior to the automated operation by Cellbot, a cryovial containing immortalized human keratinocyte (HaCaT) cells was thawed in a water bath (37 °C) for 2 min and then carefully placed in the designated tube holder. In parallel, a 50 mL conical tube containing warmed DMEM medium (10% FBS and 1% Pen–Strep), 1000 µL pipette tips, and a 60 mm petri dish were arranged in their respective holders. The automated cell culturing process was then initiated as per the programmed instructions. To assess the performance of Cellbot compared to manual labor, an operational time measurement was conducted. A timer was set to record the time taken by Cellbot to conduct the cell culturing, and the same process was replicated by a trained human labor. The time commenced from the first movement of the robot and human and concluded when the petri dish containing cells was placed inside the incubator. The incubator maintained a temperature of 37 °C with 5% CO_2 for optimal cell growth. We would like to note that conducting experiments on the robotic arm platform, a sizable mechanical device, posed challenges in the confined space of the cell culture room. Consequently, we relocated the robotic arm platform to a separate room, limiting human access to mitigate contamination risks. We maintained the cleanliness of the incubator and regularly sterilized all mechanical devices in direct contact with the cells. In the actual experiments with the robotic arm, we verified the absence of contamination in the incubator due to the robotic arm.

Following an overnight incubation period, the attached cells were examined under a light microscope, and images were captured from three random areas. Image analysis using ImageJ software was performed on the captured cell images on two consecutive days post cell culturing to determine the cell numbers. In a similar way, the automated Cellbot was utilized for cell passaging or subculturing, which involved a series of steps, including PBS washing, suction, trypsinization, and division of cells into fresh medium.

Automated $\alpha_5\beta_1$ Overexpression via Transduction: One day prior to the transduction (day 0), a HaCaT cell culture was prepared at a density of 3×10^5 cells mL^{-1} in DMEM medium supplemented with 10% FBS and 1% Pen—Strep. On the day of transduction (day 1), the HaCaT cells were exposed to polybrene at a concentration of 5 µg mL^{-1} for 1 h to enhance the efficiency of lentiviral transduction. Subsequently, the polybrene-containing medium was removed, and the cells were incubated with serum and antibiotic-free medium containing $\alpha_5\beta_1$ lentivirus at a multiplicity of infection of 10. The cell culture dish was gently shaken to ensure uniform distribution of the lentivirus and then incubated for overnight.[21] On day 2, the lentivirus-containing medium was replaced with fresh culture medium, and the cells were further incubated overnight. On the third day, the transduced HaCaT cells were observed using a Confocal Leica SP-8 microscope (Leica Microsystems, Germany), and images were captured from three different areas of the culture dish. The $\alpha_5\beta_1$ overexpressed cells produced enhanced green fluorescent protein (EGFP) as a marker of successful transduction. The EGFP positive cells were counted using ImageJ software. The time taken for transduction method was also recorded and compared between Cellbot and a trained human labor.

Supporting Information

Supporting Information is available from the Wiley Online Library or from the author.

Acknowledgements

J.H. and S.L. contributed equally to this work. This work was supported by the Basic Research Program (grant no. 2018R1A6A1A03024940) of the Ministry of Education and the Training Program of CCUS for the Green Growth (grant no. 20214000000500) of the Korea government (MOTIE).

Conflict of Interest

The authors declare no conflict of interest.

Data Availability Statement

The data that support the findings of this study are available in the supplementary material of this article.

Keywords

autonomous experiments, cell biology, robot arms

Received: September 15, 2023
Revised: December 10, 2023
Published online: February 1, 2024

[1] Q. Wu, Y. Liu, C. J. I. W. C. Wu, *ITM Web of Conf.* **2018**, *17*, 03019.
[2] C. Lytridis, V. G. Kaburlasos, T. Pachidis, M. Manios, E. Vrochidou, T. Kalampokas, S. Chatzistamatis, *Agronomy* **2021**, *11*, 1818.
[3] I. Karabegović, E. Karabegović, M. Mahmić, E. J. A. I. P. E. Husak, *Management* **2015**, *10*, 185.
[4] H. A. F. Almurib, H. F. Al-Qrimli, N. Kumar, *presented at 2011 Ninth Int. Conf. on ICT and Knowledge Engineering*, Bangkok, January **2012**.
[5] L. D. Evjemo, T. Gjerstad, E. I. Grøtli, G. Sziebig, *Curr. Rob. Rep.* **2020**, *1*, 35.
[6] B. N. Staub, S. S. Sadrameli, *J. Spine Surg.* **2019**, *5*, S31.
[7] M. Dong, Y. Zhou, J. Li, X. Rong, W. Fan, X. Zhou, Y. Kong, *J. NeuroEng. Rehabil.* **2021**, *18*, 52.
[8] M. S. A. Mahmud, M. S. Z. Abidin, A. A. Emmanuel, H. S. Hasan, *Appl. Modell. Simul.* **2020**, *4*, 130.
[9] R. Luo, C. Wang, E. Schwarm, C. Keil, E. Mendoza, P. Kaveti, S. Alt, H. Singh, T. Padir, J. P. Whitney, *presented at 2022 IEEE/RSJ Int. Conf. on Intelligent Robots and Systems (IROS)*, Kyoto, October **2022**.
[10] C. W. Coley, D. A. Thomas, J. A. M. Lummiss, J. N. Jaworski, C. P. Breen, V. Schultz, T. Hart, J. S. Fishman, L. Rogers, H. Gao, R. W. Hicklin, P. P. Plehiers, J. Byington, J. S. Piotti, W. H. Green, A. J. Hart, T. F. Jamison, K. F. Jensen, *Science* **2019**, *365*, aax1566.
[11] B. Burger, P. M. Maffettone, V. V. Gusev, C. M. Aitchison, Y. Bai, X. Wang, X. Li, B. M. Alston, B. Li, R. Clowes, N. Rankin, B. Harris, R. S. Sprick, A. I. Cooper, *Nature* **2020**, *583*, 237.
[12] L. C. Gerber, A. Calasanz-Kaiser, L. Hyman, K. Voitiuk, U. Patil, I. H. Riedel-Kruse, *PLoS Biol.* **2017**, *15*, 2001413.
[13] E. Li, A. T. Lam, T. Fuhrmann, L. Erikson, M. Wirth, M. L. Miller, P. Blikstein, I. H. Riedel-Kruse, *Plos One* **2022**, *17*, 0275688.
[14] D. Knobbe, H. Zwirnmann, M. Eckhoff, S. Haddadin, *presented at 2022 IEEE/RSJ Int. Conf. on Intelligent Robots and Systems (IROS)* , Kyoto, October **2022**.
[15] C. Stanton, A. Bogdanovych, E. Ratanasena, *presented at Proc. Australasian Conf. on Robotics and Automation*, Wellington, December **2012**.
[16] J. Arents, M. Greitans, *Appl. Sci.* **2022**, *12*, 937.
[17] W. Montalvo, J. Escobar-Naranjo, C. A. Garcia, M. V. Garcia, *Appl. Sci.* **2020**, *10*, 3823.
[18] I. Holland, J. A. Davies, *Front. Bioeng. Biotechnol.* **2020**, *8*, 571777.
[19] R. J. Lobb, M. Becker, S. Wen Wen, C. S. F. Wong, A. P. Wiegmans, A. Leimgruber, A. Möller, *J. Extracell. Vesicles* **2015**, *4*, 27031.
[20] R. J. Geraghty, A. Capes-Davis, J. M. Davis, J. Downward, R. I. Freshney, I. Knezevic, R. Lovell-Badge, J. R. W. Masters, J. Meredith, G. N. Stacey, P. Thraves, M. Vias, *Br. J. Cancer* **2014**, *111*, 1021.
[21] O. Dauwalder, L. Landrieve, F. Laurent, M. de Montclos, F. Vandenesch, G. Lina, *Clin. Microbiol. Infect.* **2016**, *22*, 236.
[22] N. Rokbani, B. Neji, M. Slim, S. Mirjalili, R. Ghandour, *Appl. Sci.* **2022**, *12*, 7091.
[23] S. Skou, R. E. Gillilan, N. J. N. P. Ando, *Nat. Protoc.* **2014**, *9*, 1727.
[24] G. Johnson, T. Nolan, S. A. Bustin, *Methods Mol. Biol.* **2013**, *943*, 1.
[25] A. J. Ninfa, D. P. Ballou, M. Benore, *Fundamental Laboratory Approaches for Biochemistry and Biotechnology*, John Wiley & Sons, Hoboken, NJ **2009**.
[26] J. C. Cox, A. D. Ellington, *Bioorg. Med. Chem.* **2001**, *9*, 2525.
[27] Z. Wang, T. Hisatomi, R. Li, K. Sayama, G. Liu, K. Domen, C. Li, L. Wang, *Joule* **2021**, *5*, 344.